Available online at www.sciencedirect.com
ScienceDirect
International Journal of Heat and Mass Transfer 51 (2008) 4109–4120
International Journal of HEAT and MASS TRANSFER
www.elsevier.com/locate/ijhmt

Vertical buoyancy preserving and non-preserving fountains, in a homogeneous calm ambient

Panos N. Papanicolaou *, Thanos J. Kokkalis

Hydromechanics and Environmental Engineering Laboratory, Department of Civil Engineering, University of Thessaly, Pedion Areos, 38334 Volos, Greece

Received 9 November 2006
Available online 18 March 2008

Abstract

Experiments were conducted on the maximum and terminal penetration depths of fountains of light fluid, issuing vertically downwards into quiescent denser fluid. Fresh water jets into saltwater, and hot water jets into fresh cold water were investigated. The source Richardson numbers extended from 0.01 (jets) to 1 (plumes). Circular and three other different shape nozzles have been employed. The normalized penetration depth is constant for jets, while it decays exponentially in plumes. Numerical evaluation of the penetration depth has indicated the need for reevaluation of the entrainment coefficient, in negatively buoyant jets.

Keywords: Buoyant jet; Negative buoyancy; Fountain; Mixing; Penetration depth; Modelling

1. Introduction

The treated liquid or gas wastes of many societies are naturally ubiquitous in diluted form. For these, a rapid discharge to the environment is often the best way of recycling. The initial dilution can be accomplished by means of turbulent buoyant jets and plumes, because they entrain large volumes of ambient fluid and mix it with the discharge fluid. The actual discharge arrangement can often be as simple as the open end of a submerged pipe. In many cases though much thought and expense must be given to design a structure, which enables us to achieve much higher initial dilution, in order to minimize the immediate effect of the discharge on the environment. The discharge devices which can be either man made ocean outfalls, or chimney stacks, or natural deep water sea vents, are usually positioned at the lowest point of the receiving fluid. The discharged fluid density is generally different from that of the receptor which is due to either different temperature or chemical composition, or to suspended particles. The resulting buoyancy forces can have a great effect on both the mean flow and mixing characteristics. Researchers have tried to understand the fundamental physical mechanisms governing turbulent buoyant jets and plumes for the past five decades. They have also developed methods to predict these flows.

The jet fluid is usually lighter and therefore positively buoyant, meaning that it can move vertically upwards. In many cases though, the density of the discharged fluid may be greater from that of the receiving fluid. Positively buoyant jets and plumes in a uniform calm ambient have been investigated thoroughly since the pioneering works of Rouse et al. [1] and Morton et al. [2]. Their flow field properties have been measured in the full range, jets, plumes and transition by Papanicolaou [3] and Wang and Law [4], and accurate models for their prediction have been developed by List and Imberger [5], Muellenhof et al. [6], Wood et al. [7], and Jirka [8], using the experimental data of the previous investigations. In all models the entrainment coefficients and jet growth characteristics measured in positively buoyant jets, verify the experiments quite accurately.

* Corresponding author.
E-mail address: panospap@uth.gr (P.N. Papanicolaou).

0017-9310/$ - see front matter © 2008 Elsevier Ltd. All rights reserved.
doi:10.1016/j.ijheatmasstransfer.2007.12.023

Nomenclature

A	cross-section area
B	initial specific buoyancy flux at the nozzle
b_c	jet lateral dimension where $\Delta\rho(z,r) = (1/e)\Delta\rho(z,0)$
b_w	jet lateral dimension where $w(z,r) = (1/e)w(z,0)$
C	constant of proportionality
C_p	jet width parameter
D	jet diameter
e	base of Neperian logarithm, 2.718...
F_0	initial jet Froude number
g	gravitational acceleration
g'_0	$[(\rho_a - \rho_0)/\rho_0]g$
l_M	characteristic length scale, $M^{3/4}/B^{1/2}$
l_Q	characteristic length scale, $Q/M^{1/2}$
$m(z)$	specific momentum flux at distance z
M	initial specific momentum flux at the nozzle
Q	initial volume flux at the nozzle
r	radial distance from axis
R	hydraulic radius
Re	Reynolds number
R_0	initial jet Richardson number
R_p	plume Richardson number
$R(z)$	Richardson number at distance z
S	average dilution, $\mu(z)/Q$
t	time
T_0	jet temperature
T_a	ambient temperature
$T(z)$	average over the cross-section temperature
$w(z,r)$	time-averaged axial velocity at (z,r)
W	jet exit velocity
z	vertical distance from nozzle
z_0	location of the jet virtual origin
Z	terminal penetration depth
Z_{max}	maximum penetration depth

Greek symbols

α	entrainment coefficient
$\beta(z)$	specific buoyancy flux at distance z
$\Delta\rho_0$	$\rho_a - \rho_0$
$\Delta\rho(z,r)$	$\rho_a - \rho(z,r)$
$\Delta\rho(z)$	$\rho_a - \rho(z)$
ΔT_0	$T_0 - T_a$
$\Delta T(z)$	$T(z) - T_a$
λ	b_c/b_w
$\mu(z)$	volume flux at distance z
$\rho(z,r)$	jet time-averaged density at (z,r)
$\rho(z)$	average over the cross-section density

Superscripts and subscripts

$()_{0,j}$	jet characteristic value
$()_p$	plume characteristic value
$()_a$	ambient fluid characteristic value
$()_c$	characteristic value at centerline

Negatively buoyant jets for which gravity forces oppose their movement, are called fountains. Turbulent fountains are formed when a continuous jet of dense fluid is injected rapidly upwards into a less dense environment, or when a continuous jet of buoyant fluid is injected downwards, into a denser environment (see [9–11]). They arise in a number of important situations both in engineering and in nature. Applications include the forced heating or cooling of large enclosures, such as large assembly line factory spaces, and buildings or rooms. During the heating or cooling of a room, a jet of air at different temperature may be forced into the room through a floor or ceiling vent. Other applications include the disposal of brines or heavier industrial wastes into the ocean, and the improvement of water quality by forced mixing in reservoirs, small lakes and harbors, or fjords. Jet mixing in a tank is used industrially to blend fresh fluid with the contents of a tank. Geophysical buoyant jets resulting from temperature (or salinity) differences can occur in the ocean and in magma chambers near the crust of the earth. Other examples of natural fountains are the evolution of volcanic eruption columns investigated by Woods and Caufield [12], and the replenishment of magma chambers in the Earth's crust by Turner and Campbell [13] and Campbell and Turner [14].

Turbulent fountains in a uniform calm ambient have been investigated for a long time since Turner's [9] pioneering work. The mechanics of their mixing is of great interest for design engineers, who desire to optimize the dilution of heavier fluid into a volume of lighter one. The turbulent jet behavior depends on three groups of factors: (i) jet parameters, (ii) environmental parameters, and (iii) geometrical factors. The first group includes the initial jet velocity distribution and turbulence level, the jet mass, momentum, and tracer (such as heat, salinity, or contaminant) flux. The second group of variables includes the ambient fluid parameters, such as turbulence level, currents, and density stratification. These factors usually begin to influence jet behavior at some distance from the orifice. The geometrical factors include the jet shape, its orientation and proximity to solid boundaries or to the free surface.

Negatively buoyant jets are somewhat more interesting than positively buoyant ones, because the buoyancy force and momentum compete. Very little is known about the transient character of negatively buoyant jets upon start-up. Their mechanics is more complicated by the fact that buoyancy is acting in a direction opposite to that of the initial flow. Therefore, the reversing buoyancy reduces the flux of momentum, and the vertical velocity vanishes at

some distance from the source. The jet reaches its maximum penetration length soon after startup then it reverses its direction and flows back onto itself as a fountain. Turner [9] showed that the properties of a vertical dense jet issuing vertically upwards from a small source into a calm uniform environment are mainly governed by the initial specific jet momentum and buoyancy fluxes. The turbulent interaction between the up-flow and down-flow restricts the rise of fluid any further, thus immediately reducing the initial fountain height to a smaller terminal value. This observed final height was related to the momentum and buoyancy fluxes at the source, using dimensional arguments. The finding was that the terminal, steady state jet penetration normalized by the jet diameter, varied linearly with the initial densimetric Froude number, and it was verified experimentally. Several investigations have been completed since, regarding vertical negatively buoyant jets in a motionless uniform ambient. Temperature measurements have been performed by Seban et al. [15] in a heated air-jet discharged downwards. The stable stratification formed by a fountain has been studied by Baines et al. [11], once it falls back and spreads along the floor of the dispersion chamber, re-entraining some of the already mixed heavier fluid. Measurements of the penetration height of fountains have been reported by Demetriou [16] and Zhang and Baddour [17], for a wide range of initial densimetric Froude numbers. The effects of cross flows and angle of injection on negatively buoyant jets have been studied by Lindberg [18]. Pantzlaff and Lueptow [19] investigated the evolution (transient character from startup to steady state) of positively and negatively buoyant jets. They have applied laser induced fluorescence imaging, and particle image velocimetry, to study the velocity field of a fountain near the top and at the bottom of a tank. Recently, Bloomfield and Kerr [20] have reported measurements of a vertical fountain out of a pipe, regarding the maximum and terminal penetration heights in a uniform calm ambient.

1.1. Dimensional arguments – review of earlier experiments

Consider a jet of lighter fluid, issuing vertically downwards from a 'point' source, into a homogeneous calm ambient of higher density. We assume that the jet starts abruptly discharging constant volume flux of lighter fluid. During the early stages of the flow (transient period), the jet mixes with heavier ambient fluid, which applies an opposing (buoyancy) force to the jet fluid, that reaches a maximum depth Z_{max}. Then, it folds up forming an up-flow region which surrounds the down-flow region of the jet. The result is that the down-flow jet mixes with the heavier up-flow fluid, applying an opposing momentum which results in a lower, steady state, terminal penetration depth Z. Full description of the mechanics of jets with reversing buoyancy has been presented by Turner [9].

The terminal, steady state vertical penetration depth Z of the jet, depends upon the variables characterizing the source conditions. Ignoring viscosity (the jet is assumed to be turbulent), a general functional relationship for the dependent variable Z is

$$Z = f(Q, M, B). \tag{1}$$

Q is the source volume (specific mass) flux, M and B are the specific momentum and buoyancy fluxes, respectively, computed as

$$Q = \frac{\pi D^2}{4} W, \quad M = QW, \quad B = \frac{\rho_a - \rho_0}{\rho_0} gQ = g'_0 Q. \tag{2}$$

In the above relationships, D is the jet diameter, W is the uniform jet velocity at the nozzle, g is the gravitational acceleration, ρ_0 and ρ_a are the jet and ambient fluid densities, respectively.

Fischer et al. [21] have defined two length scales based upon the initial kinematic buoyant jet characteristics as

$$l_Q = \frac{Q}{M^{1/2}} \quad \text{and} \quad l_M = \frac{M^{3/4}}{B^{1/2}}. \tag{3}$$

Their ratio l_Q/l_M is defined to be the initial buoyant jet Richardson number R_0

$$R_0 = \frac{l_Q}{l_M} = \frac{QB^{1/2}}{M^{3/4}} = \left(\frac{\pi}{4}\right)^{1/4} \frac{\sqrt{g'_0 D}}{W}, \tag{4}$$

which is inversely proportional to the initial jet densimetric Froude number $F_0 = W/\sqrt{g'_0 D}$.

From Eq. (1), using Eqs. (3) and (4), we may deduce two dimensionless terms, the terminal normalized penetration depth Z/l_M or Z/l_Q and the initial jet Richardson number R_0. Thus Eq. (1) may be written as

$$\frac{Z}{l_Q} = f(R_0) \quad \text{or} \quad \frac{Z}{l_M} = f(R_0). \tag{5}$$

In case that the initial jet momentum flux M is large enough, if compared to the buoyancy flux B (R_0 is small, jet-like flow), we may ignore the source volumetric discharge Q, since the local volume flow rate $\mu(Z) \gg Q$. Thus $Z = f(M, B)$ and by dimensional arguments of Turner [9]

$$\frac{Z}{l_M} = C, \tag{6}$$

C being a constant. Applying the same dimensional arguments, the maximum penetration depth Z_{max} can be scaled accordingly

$$\frac{Z_{max}}{l_Q} = f(R_0) \quad \text{or} \quad \frac{Z_{max}}{l_M} = f(R_0), \tag{7}$$

while for initially jet-like flows (small R_0), neglecting Q the ratio Z_{max}/l_M, must also be a constant.

Earlier investigators have used different representations of Eq. (6) to determine the constant of proportionality. We have reworked the experimental data and we have reevaluated the proportionality constants. In Fig. 1 we have plotted all the data collected by earlier investigations, using the same dimensionless variables Z/l_M and R_0, while in Table 1 we tabulate the constants calculated from avail-

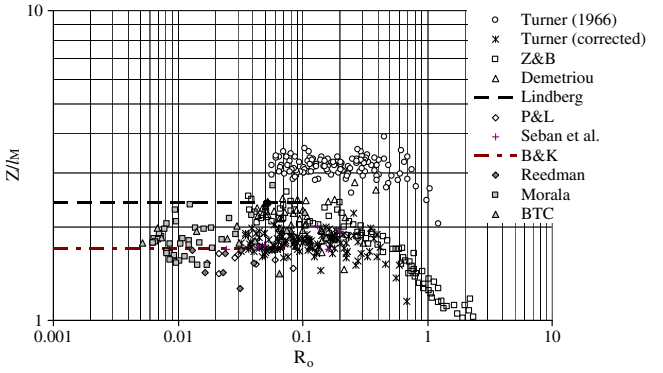

Fig. 1. Normalized penetration heights reported in earlier experiments, plotted against the initial jet Richardson number R_0.

Table 1
Normalized penetration heights reported in earlier experimental investigations

Investigator	Z_{max}/l_M	Z/l_M
Turner [9]	–	1.77 (3.17)
Seban et al. [15]	–	1.86
Demetriou [16]	2.625	2.18
Morala [11]	–	1.84
Reedman [11]	–	1.53
Baines et al. [11]	–	1.87
Lindberg [18]	–	2.40
Zhang and Baddour [17]	–	2.11
Pantzlaff and Lueptow [19]	–	1.57
Bloomfield and Kerr [20]	2.325	1.71

The constant in parenthesis corresponds to Turner's uncorrected data.

able data. The data used are from Turner [9], Baines et al. [11], Seban et al. [15], Demetriou [16], Zhang and Baddour [17], Pantzlaff and Lueptow [19], Lindberg [18] and Bloomfield and Kerr [20]. The data referred to as Reedman and Morala have been copied from Baines et al. [11]. In the data published by Lindberg [18] and Bloomfield and Kerr [20], there is no information regarding the initial jet Richardson number R_0, therefore we plot two lines at $C = 2.40$ and 1.71, respectively. The data from Turner [9] have been corrected since Turner indicated $C = 1.85$, while from Fig. 5 of the reference, the constant of proportionality is noticeably higher ($C > 3$).

From Table 1, we may note that the constant of proportionality is quite different in each investigation. The average value of C is 2.19, while the standard deviation is 0.57, which is quite high. This may be due to the fact that either the initial buoyant jet parameters have been miscalculated, or the experimental tanks that were quite different in size (Table 2) have had an effect on the flow. The experimental constants regarding both, Z_{max} and Z are quite equivocal, since different authors propose different constants. We believe that the discrepancy may be due to errors made from the following factors:

1. Geometrical, related to the size of the mixing tank, if compared to the jet spreading width. In Table 2 we summarize the size of mixing tanks used in different experiments. The side walls of narrow tanks may interfere with jet spreading more than those of wider tanks. The jet size (visual width) is approximately $4b_c \approx 0.50z$, b_c being the $1/e$ width based upon the time-averaged jet concentration profile [3] and z the distance from the nozzle. The mechanics of the jet is affected by the induced recirculation in the tank. If the jet is close to the tank walls, the recirculating flow applies shear stress to the jet boundary, thus altering its momentum flux. For centered jets with widths not exceeding 25% of the horizontal dimension of the tank, the recirculation effect is minimized.
2. Initial jet parameter estimates, such as the jet volume flux, momentum and buoyancy fluxes. We think that the error in the measurement of the volume and buoyancy fluxes is the same in all experiments, since the flow meters used and the accuracy in density measurement are quite standard. There may be some problem in the initial momentum estimate, since the velocity profile at the jet exit has not been measured. Jets out of nozzles at reasonably large Reynolds numbers have more or less uniform velocity profiles [22], and the initial momentum can be accurately estimated. Jets out of pipes, especially those at low Reynolds numbers, have greater momentum than that with uniform exit velocity distribution.
3. Error in the length estimates from pictures or images of the flow. The penetration depths are estimated from the flow images such as pictures, shadowgraphs or laser tomography via induced fluorescence. Once the scale is determined, laser tomography gives the most accurate length measurements. Photography of dyed jets and shadowgraphs may be affected by the refractive index differences between the air, glass and mixing tank liquid.

Table 2
Dimensions of the dispersion tanks (m) used in earlier experiments

Author	Cross-section	Depth
Turner [9]	0.45×0.45	1.40
Demetriou [16]	1.20×1.20	1.55
Lindberg [18]	3.64×0.405	0.508
Zhang and Baddour [17]	1×1	1
Pantzlaff and Lueptow [19]	$D = 0.295$	0.89
Bloomfield and Kerr [20]	0.40×0.40	0.70
Present experiment	0.80×0.80	0.94

Most of the available experiments are focused on the maximum and terminal penetration heights (or depths), rather than on the description of their flow field. The measurements made by Seban et al. [15] and Pantzlaff and Lueptow [19] cannot be conclusive, since they don't give any indication of the jet flow field characteristics, such as the entrainment coefficient and the average dilution at the maximum penetration, respectively.

In the present investigation we are going to determine the constant of proportionality C from experiments of two types of fountains, with or without preserving buoyancy. We are also going to report data regarding the maximum

penetration (wherever it is possible), as well as the transient characteristics of the fountain, before it reaches steady state. Finally, we will attempt to predict the maximum penetration via 1D modeling, using earlier data regarding the entrainment and growth of positively buoyant jets.

2. Experiments

2.1. The experimental set-up

Experiments have been carried out at the Hydromechanics and Environmental Engineering Laboratory of the University of Thessaly. The experimental apparatus was a 94 cm deep tank made of 1.25 cm thick glass, with square cross-section 80 cm × 80 cm.

A jet of lighter fluid pointing vertically downwards was positioned near the free surface at the center of the tank cross-section. The jet plenum consisted of a 25 cm long, 4 cm i.d. PVC tube, part of which was filled with sponge followed by a 6 cm long honeycomb section. Thus, possible large eddies which might affect the jet initial conditions were destructed and the flow was straightened. A flexible supply tube was mounted at its entrance section, and the jet nozzles were mounted at its exit section. Four round nozzles of 0.5, 1, 1.5 and 2 cm in diameter have been used, along with three different shape nozzles, a square, a triangular with equal sides and an orthogonal with a 2:1 side ratio, all of them with rounded corners. The jet nozzle elevation was set around 10 cm below the free surface. In the present experiment we ensured that the jet width did not exceed 25% of the horizontal tank dimension (jet maximum rise height was lower than 40–50 cm), thus 'eliminating' the unnecessary shear due to the recirculation inside the tank.

Two sets of experiments have been conducted. One where the initial jet specific buoyancy flux was conserved, and one where it decayed. For the first set of experiments, the tank was filled with saltwater at the desired density, while the jet fluid was fresh, tap water. A constant head tank was used as the jet supply in order to obtain the desired steady discharge of light fluid throughout the experiment. The tank fluid was stirred to become homogeneous and allowed to settle for about 20 min prior to a test. The temperatures of the jet freshwater and tank saltwater were practically identical, close to the room temperature, to minimize thermal effects on the flow. The density difference between jet and ambient fluid, the jet diameter and discharge were chosen properly, in order to obtain the desired initial jet Richardson number R_0. Throughout a test, the fresh water jet discharge was controlled by a precision vane, and monitored with a system of three flow meters. In the first set of experiments, all different nozzle shapes have been used for comparison.

For the second set of experiments, we filled the tank with fresh water, while the jet fluid was hot water. The hot water supply consists of an electric water heater with a recirculation pump, used to make the jet fluid homogeneous. The water heater was pressurized before each test, and the jet inlet tube was properly insulated. The jet fluid was bypassed and disposed, until a temperature sensor at the jet plenum entrance showed constant temperature for the jet fluid. Then the test started. The desired initial jet Richardson number for each test was obtained by varying appropriately the jet temperature (density), diameter, and discharge. The flow rate was controlled by the same system of flow meters, used for the first set of experiments. In the second set of experiments, only round nozzles have been used.

The fountain flow was made visible by the standard shadowgraph technique. Using a slide projector as a light source, the jet flow field was projected on semitransparent white paper along with two square grids 5 cm × 5 cm drawn on the two opposite side glasses of the tank, that are normal to the direction of the beam of light. The jet flow field image was recorded with a digital video camera at a rate of 25 fps. This procedure allowed for the fountain heights to be measured on each frame, and an average value of the fluctuating terminal height to be estimated over a period of time. From each frame, the penetration depth was estimated as the average value measured in both grid systems. From optical calculations neglecting the glass panel thickness, considering the refraction of the projection rays, we have come to the following conclusions: (1) The projected grid spacing was square within 1 mm, when the light projector was positioned at a distance greater than 4 m from the front glass panel. (2) Errors in the penetration depth estimate did not exceed 0.3 cm, in case it did not occur at the jet axis but at distances $r = \pm 5$ cm off axis.

2.2. Parameters used in the experiments

A large number of experiments were conducted by Kokkalis [23] to investigate the penetration depths in the full

Table 3
Range of the experimental parameters used in saltwater jets with different nozzle sections, and in heated round jets

Nozzle	Round	Orthogonal	Square	Triangular	Round-Hot
# runs	46	15	12	11	23
D, R (cm)	0.5, 1.0, 1.5, 2.0	0.277	0.265	0.256	0.5, 1.0, 1.5, 2.0
ρ_a (g/cm^3)	1.007–1.021	1.006–1.023	1.006–1.023	1.006–1.023	0.9965–0.9973
ρ_0 (g/cm^3)	0.995–0.997	0.995–0.996	0.995–0.996	0.995–0.996	0.9757–0.9866
Re	770–5840	745–4540	900–5500	900–5440	1030–15,370
R_0	0.016–0.973	0.071–0.632	0.052–0.469	0.054–0.455	0.019–0.797

range of initial jet Richardson numbers R_0. In the fresh water–salt water experiments all different types of nozzles were used besides the circular ones, while in the hot–cold water experiments only jets out of round nozzles were investigated. The jet nozzle diameter (or the hydraulic radius R, for non-circular nozzles), and the range of the basic experimental parameters are summarized in Table 3. One may note that the initial buoyant jet Reynolds numbers exceeded 700, meaning that the transition to turbulence occurred within five jet diameters from the nozzle. Also, the initial jet Richardson numbers R_0 in fresh and hot water circular jets extend in the full range, from very small (0.016) corresponding to initially jet-like flow to about 1 for plumes, because of the flexibility of using round nozzles with four different diameters. The R_0 range in the non-circular nozzles was limited to values above 0.05, because there was only one nozzle of a kind available.

3. Results and discussion

The finite volume of the tank did not appear to affect the transient character of the buoyant jet, because the jet is far from the side walls, and it disperses as if it were in an unbounded ambient. Flow visualization of the transient character of a negatively buoyant jet is shown in Fig. 2. The jet initially penetrates downward into the dense liquid in Fig. 2a. Then it reaches the maximum penetration depth Z_{max} in Fig. 2b, as the momentum flux vanishes. Subsequently, the flow reverses in the upward-moving annular region in Fig. 2c, and decreasingly it reaches steady state, oscillating around the terminal penetration depth Z, in Fig. 2d. The upward momentum is not large enough, to eliminate the downward flow from the nozzle. Looking at the videos from the experiments, we have noticed that no reverse flow reaches the elevation of the nozzle, before the front has reached the maximum penetration depth, regardless of the initial jet Richardson number. The transient behavior of turbulent fountains has also been discussed by Turner [9] and Pantzlaff and Lueptow [19].

The oscillation of steady state penetration depth can be clearly observed in Fig. 3, depicting the temporal evolution of the terminal depth. It is evident that following the abrupt start-up, the jet reaches the maximum penetration depth Z_m, after a short time. Following Pantzlaff and

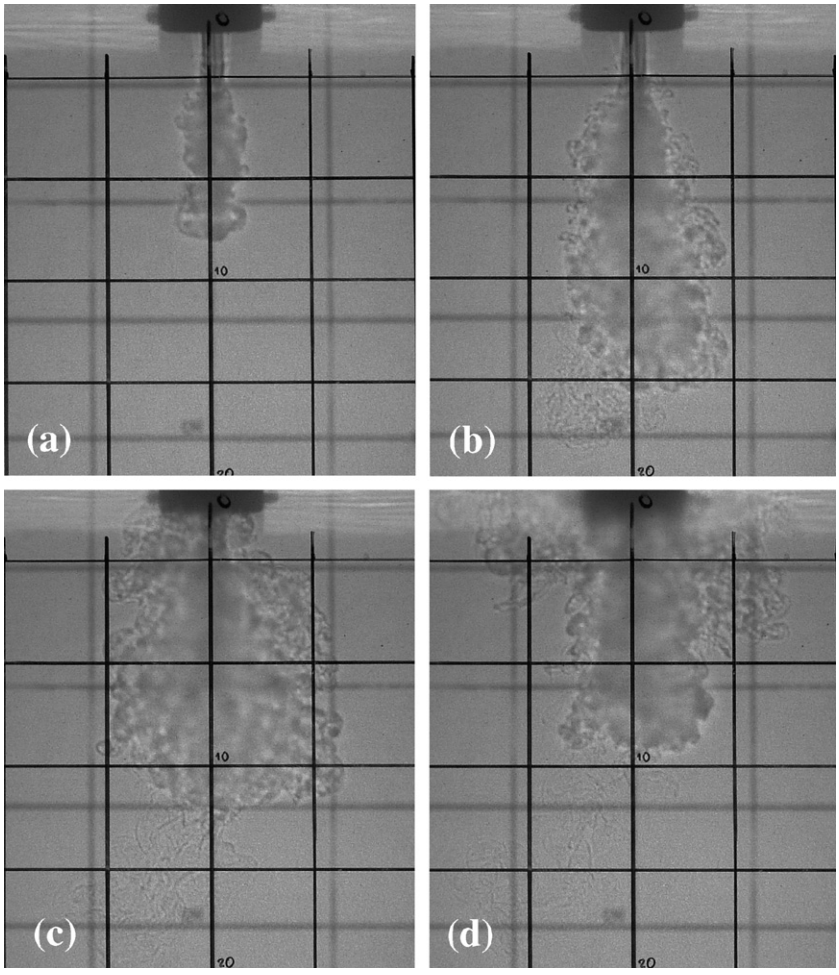

Fig. 2. Sequence of photos taken from (a) a starting buoyant jet, (b) at the maximum penetration depth Z_{max}, (c) descending flow, and (d) at the terminal, steady state, penetration depth Z. Buoyant jet parameters are: $D = 1$ cm, $\Delta\rho = 14$ g/l, $W = 19.95$ cm/s, $R_0 = 0.173$.

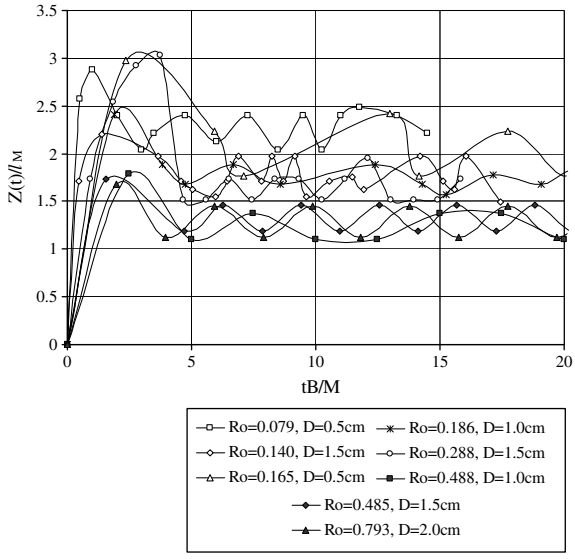

Fig. 3. Time evolution of the normalized penetration depth Z/l_M versus the normalized time $t(B/M)$ from startup.

Lueptow [19], we have plotted the dimensionless penetration depth $Z(t)/l_M$ versus the normalized time $t(B/M)$ for round jets of different diameters at different initial Richardson numbers. We observe that the maximum penetration depth occurred at times that are lower than 5, while at greater times it oscillated around a mean, steady state terminal value. For higher initial Richardson numbers (greater than 0.1), we observe that the terminal normalized penetration depth is lower than 2, while for jet-like flows it is around 2. In the heated jet we could not record the maximum penetration depth, because of the transient jet temperature during the startup of each experiment. At higher initial Richardson numbers when the buoyant jet is plume-like, the penetration depth is quite limited and mixing with ambient fluid is marginal. The frequency of oscillation is a function of the jet nozzle diameter, given that the flow consists of 'periodic' large eddies, the frequency of which depends upon the natural frequency of eddies forming at the nozzle and the distance Z from it.

3.1. Terminal penetration depth

The normalized maximum and terminal penetration depths of round (buoyancy preserving) negatively buoyant jets is plotted in Fig. 4 as a function of the initial Richardson number R_0. When R_0 is lower than 0.2, the normalized penetration depths Z/l_M and Z_{max}/l_M seem to take constant values around 2.0 and 3.0, respectively, result which is congruent with dimensional analysis. When R_0 is greater than 0.3, both penetration depths are drastically reduced. Therefore, for round vertical fountains we may state that the terminal penetration depth oscillates around a distance $2l_M$ from the nozzle, while $Z_{max} \approx 3l_M$. The experimental values obtained in the present investigation are higher from that of Turner's [9] corrected data, similar to those

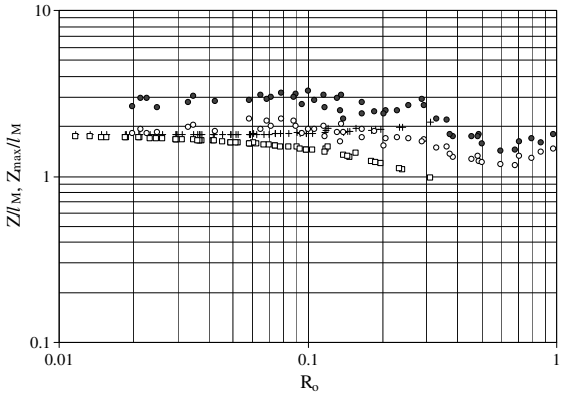

Fig. 4. Round salt water (buoyancy preserving) jets. Normalized maximum (solid circles), terminal penetration depths (open circles), maximum terminal depth model predictions when $z_0 = 0$ (squares) and $z_0 = 3.28D$ (crosses).

reported by Demetriou [16] and Zhang and Baddour [17], and higher from those measured by Pantzlaff and Lueptow [19] and Bloomfield and Kerr [20]. We believe that a value of constant C around 2 is reasonable, because the tanks used in the present investigation and those by Demetriou [16] and Zhang and Baddour [17], are of about the same size. They are quite large, with minimal boundary effects on the dynamics of the negatively buoyant jet. The measurements of Zhang and Baddour [17] were extended to $R_0 \approx 3$, initial Richardson number which is very high, meaning that the length scale l_M is a fraction of the jet nozzle diameter. Efficient mixing under these circumstances cannot be obtained since $Z/l_M < 1$, meaning that jet penetration does not exceed one jet diameter.

In a vertical hot water round jet with reversing buoyancy, the initial jet buoyancy flux cannot be preserved. When the jet mixes with ambient fluid, its temperature and subsequently the coefficient of thermal expansion of water is reduced, resulting in reduced local buoyancy flux. Therefore, the buoyancy force opposing the jet movement is reduced. One could expect a dramatic increase of coefficient C in Eq. (6), but this is not the case. Plotting the normalized penetration depth Z/l_M as a function of R_0, we can observe in Fig. 5 that for R_0 lower than 0.3, $C \approx 2$. This is

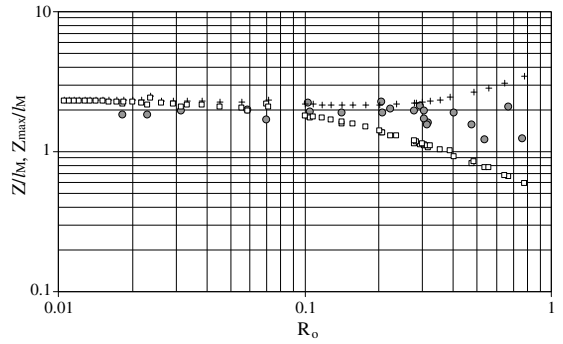

Fig. 5. Round hot water jets. Normalized terminal penetration depths (solid circles), maximum terminal depth model predictions when $z_0 = 0$ (squares) and $z_0 = 3.28D$ (crosses).

not any different from the constant we obtained for round fresh water jets in saltwater. Thus, we can state that hot water negatively buoyant jets, behave as negatively buoyant (buoyancy preserving) jets. This is probably due to the fact that the initially jet-like flow turns into plume-like after a short distance from the nozzle, and the reversing buoyancy which has already reduced the initial jet momentum flux drastically, takes over.

The maximum penetration depth in the case of hot water jets could not be obtained, since the jet plenum was initially filled with cold water before we supplied it with constant temperature hot water. After start-up, when $B = 0$, there was a transient jet of increasing temperature, thus increasing B for a short time, during which l_M was not constant. Therefore, $Z_{\max}$ could not be obtained, while Z was obtained once the jet temperature became constant. It is evident from Fig. 5 that the constant C is reduced, when $R_0 > 0.3$.

The results regarding buoyancy preserving non-circular jets are plotted in Fig. 6, where we have plotted Z/l_M and $Z_{\max}/l_M$ versus R_0, for jets with orthogonal, square and triangular sections. They are limited to R_0 greater than 0.05, since there was only one size available for each nozzle. It would be of interest to investigate the full range of initial Richardson numbers. From the available data, one may observe that negatively buoyant jets with triangular and square nozzle sections penetrate around two characteristic lengths ($2l_M$) into the ambient, while the maximum penetration is slightly below $3l_M$. The jets with an orthogonal 2:1 nozzle section penetrate at shorter depths, meaning that they entrain more ambient fluid than the circular, square or triangular ones. Buoyant jets from the same orthogonal nozzle in a linear density gradient investigated by Konstantinidou and Papanicolaou [24], have shown similar behavior, since the elevation of lateral spreading was lower, if compared to that for round jets. Elliptical pure jets with 2:1 axis ratio have also been reported by Ho and Gutmark [25] to entrain ambient fluid at higher rates, if compared to the round ones. This must be investigated in greater detail, and it might be a suggestion towards the direction of enhancing mixing by buoyant jets, using nozzle shapes that are more efficient than the axisymmetric ones. From Fig. 6, it is evident that the normalized maximum penetration depth is reduced, when $R_0 > 0.3$.

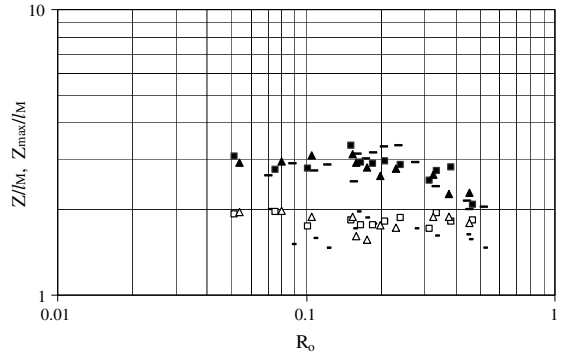

Fig. 6. Non axisymmetric salt water jets. Normalized maximum and terminal penetration depths of triangular (solid triangles and open triangles), square (solid squares and open squares), and orthogonal (long bars and short bars) nozzles, respectively.

3.2. One dimensional modeling

The local specific mass, momentum and buoyancy fluxes in a vertical buoyant jet, can be computed from the time-averaged Gaussian velocity $w(r,z)$ and density deficit $\Delta\rho(r,z)$ profiles over a cross-section A as

$$\begin{aligned}\mu(z) &= \int_A w(r,z)\mathrm{d}A = \pi b^2 w,\\ m(z) &= \int_A w^2(r,z)\mathrm{d}A = \frac{\pi b^2 w^2}{2},\\ \beta(z) &= \int_A g\frac{\Delta\rho(r,z)}{\rho_0}w(r,z)\mathrm{d}A = \pi(\frac{\Delta\rho_c}{\rho_0})gwb^2\frac{\lambda^2}{1+\lambda^2}.\end{aligned} \tag{8}$$

Then, the 1D differential equations of continuity, z-momentum and buoyancy conservation are written

$$\begin{aligned}\frac{\mathrm{d}\mu}{\mathrm{d}z} &= 2\sqrt{2\pi}\alpha m^{1/2},\\ \frac{\mathrm{d}m}{\mathrm{d}z} &= \frac{1+\lambda^2}{2}\frac{\mu\beta}{m},\\ \frac{\mathrm{d}\beta}{\mathrm{d}z} &= 0,\end{aligned} \tag{9}$$

where $\lambda = b_c/b_w$ is defined to be the $1/e$ temperature or density deficiency to velocity width ratio. The initial conditions for the integration are

$$\begin{aligned}&\mu(0) = Q = \frac{\pi D^2}{4}W, \quad m(0) = M = \frac{\pi D^2}{4}W^2,\\ &\beta(0) = B = \frac{\rho_a - \rho_0}{\rho_0}gQ\end{aligned} \tag{10}$$

where W is the jet velocity at the nozzle. The theoretical flow origin can be assumed to be either at $z = 0$, or following List and Imberger [5] at a distance z_0 from the nozzle computed from the jet width parameter:

$$C_p = \frac{\mu}{zm^{1/2}} \tag{11}$$

evaluated by Papanicolaou and List [26] to be 0.27. Substituting the initial jet volume and momentum fluxes in Eq. (12) one has that

$$C_p = \frac{Q}{z_0 M^{1/2}} \Rightarrow z_0 = \frac{Q}{C_p M^{1/2}} = \frac{\ell_Q}{C_p} = \sqrt{\frac{\pi}{4}}\frac{D}{C_p} = 3.28D. \tag{12}$$

From the solution of the above system of differential equations we can only predict the maximum terminal penetration depth $Z_{\max}$, since we have not taken into account the reverse flow, so that we can predict the steady state terminal height of rise Z.

In the case of heated jets, the initial jet specific buoyancy flux cannot be conserved ($\mathrm{d}\beta/\mathrm{d}z \neq 0$), that is due to the

change of density with temperature (thermal expansion coefficient of water). For temperatures in the range of 15–65 °C, the density of tap water as a function of the temperature may be approximated by the relationship

$$\rho(T) = -0.0038T^2 - 0.0685T + 1001.05, \tag{13}$$

where T is in °C and the water density is in g/l [27]. If at a distance z from the origin the average over a cross-section temperature is $T(z)$ and the buoyancy flux is $\beta(z)$, then at distance $z+\Delta z$ they will be $T(z+\Delta z)$ and $\beta(z+\Delta z)$, respectively. Assuming heat flux conservation, one can write

$$Q\Delta T_0 \approx \mu(z)\Delta T(z), \tag{14}$$

neglecting the heat flux transported by turbulence that is 10–15% of the total [26]. Then, the corresponding buoyancy flux $\beta(z+\Delta z)$ may be computed from equation

$$\beta(z+\Delta z) = \mu(z+\Delta z)\frac{\Delta\rho(z+\Delta z)}{\rho_0}g, \tag{15}$$

where $\rho(z+\Delta z) = f[T(z+\Delta z)]$ according to the relationship presented earlier.

For the integration of the system of differential equations we can use the parameters reported by Papanicolaou and List [26] regarding the entrainment coefficient α and width ratio λ

$\alpha_j = 0.0545$ (jets) ,
$\alpha_p = 0.0875$ (plumes) ,
$\lambda_j = 1.20$ (jets),
$\lambda_p = 1.067$ (plumes).

Furthermore, the entrainment coefficient and the width ratio are assumed to be functions of the local buoyant jet Richardson number $R(z)$, and may be evaluated from equations suggested by List in Fischer et al. [21]

$$\alpha = \alpha_j \exp\left(\ln(\alpha_p/\alpha_j)\left(\frac{R(z)}{R_p}\right)^2\right) \quad \text{and}$$

$$\lambda = \lambda_j \exp\left(\ln(\lambda_p/\lambda_j)\left(\frac{R(z)}{R_p}\right)^2\right), \tag{16}$$

or alternatively by a relationship based on energy conservation, that was proposed by Priestley and Ball [28]

$$\alpha = \alpha_j - (\alpha_j - \alpha_p)\left(\frac{R(z)}{R_p}\right)^2 \quad \text{and}$$

$$\lambda = \lambda_j - (\lambda_j - \lambda_p)\left(\frac{R(z)}{R_p}\right)^2. \tag{17}$$

$R(z) = \mu(z)\beta(z)^{1/2}/m(z)^{5/4}$ is the local buoyant jet Richardson number, and $R_p = 0.63$ is the plume Richardson number, evaluated from experiments by Papanicolaou [3]. Apparently, $R(z) \to \infty$ when $m(z)$ vanishes at the terminal penetration depth. We have considered that the entrainment coefficient takes its asymptotic plume value a_p, when $R(z) > R_p$.

The system of three equations (10) with initial conditions (11) was solved using a fourth order Runge–Kutta routine. The execution of the routine was terminated, when the jet momentum flux has vanished, once it has reached the maximum penetration depth. We did not carry on simulations with reversing flow, since there is no available information regarding the negatively buoyant jet structure. The results of the computations for buoyancy preserving and heated reversing jets are shown in Figs. 4 and 5, respectively, for virtual origins located at the nozzle exit ($z_0 = 0$) and 3.28 diameters downstream from the nozzle. From the graphs one can observe that the normalized estimated maximum penetration depth is rather close to the steady state terminal penetration depth, than to the measured one for initially jet-like flows ($R_0 < 0.1$). Bloomfield and Kerr [20] have made the same computation using top-hat profiles for the mean velocity and excess density profiles and found the constant to be 2.32, result that is not congruent with the present computation, (we have obtained the same result by eliminating $\sqrt{\pi}$ from continuity equation). When $R_0 > 0.1$ one may observe that the computed penetration depth data slope upward when $z_0 = 3.28D$ and downward when $z_0 = 0$. When the flow is initially driven by both, vertical momentum and buoyancy fluxes (jet is in transition from the jet-like to plume-like), the characteristic length scale l_M is reduced, and becomes approximately equal to the jet diameter D when $R_0 \to 1$. Therefore, for $z_0 = 3.28D$, as $R_0 \to 1$ the normalized elevation of the virtual origin $z_0/l_M \to 3.3$, i.e. the virtual origin is located well above the maximum penetration depth (computed penetration data slope upward). On the other hand, when $z_0 = 0$ for $R_0 > 0.1$ we assume that ambient fluid starts to entrain from the elevation of the jet nozzle. This assumption is incorrect since we neglect the laminar jet regime in the few first diameters from the nozzle. In fact, at large initial R_0 there is essentially no mixing of the jet with ambient fluid. Therefore, the measured maximum penetration depth is bigger since the kinetic energy of the unmixed jet fluid will become potential energy at higher elevations, if compared to that reached by the slower moving jet that mixes with ambient fluid as it is assumed by our model. Practically speaking, application of negatively buoyant jets for mixing is meaningful only when $R_0 \ll 1$, meaning that the flow will initially be jet-like.

We repeated the computations using the MATLAB solver routines, and our results were verified. Computation using top-hat velocity and density (or temperature) distributions did not make an essential difference. All the results are summarized in Table 4 for low initial Richardson numbers (initially jet-like flow).

From the results listed above and the corresponding graphs of Figs. 4 and 5 one may note the constant of proportionality takes an asymptotic value at low initial Richardson numbers. The normalized rise heights start to diverge from the measurements at lower R_0 when the virtual origin coincides with the jet exit elevation, if compared to those with the virtual origin at $3.28D$ proposed by List and Imberger [5], which diverge for $R_0 > 0.10$. In a heated

Table 4
Computed normalized terminal penetration depth of jets ($R_0 < 1$), using Gaussian and top-hat distributions of the time-averaged velocity and density deficiency, when the jet origin is located at the nozzle or at 3.28 diameters downstream

Type	Profile	α_j/α_p	λ_j/λ_p	Z/l_M ($z_0 = 0$)	Z/l_M ($z_0 = 3.28D$)
Saltwater jet	Gaussian	0.0545/0.0875	1.20/1.067	1.74	1.78
Saltwater jet	Top-hat	0.076/0.120	1	1.84	1.87
Heated jet	Gaussian	0.545/0.0875	1.20/1.067	2.26	2.33

jet at 60 °C that discharges into water of 20 °C, the computed Z_{max}/l_M is found to be greater from that computed for buoyancy preserving jets as expected, since the initial buoyancy flux is drastically reduced. It has also turned out to be higher from the measured terminal penetration depth Z/l_M. This was expected since the specific buoyancy flux of the jet is reduced as it mixes with ambient fluid, due to the variation of the thermal expansion coefficient of water with temperature. Reducing the initial temperature difference further between jet and ambient fluid, the asymptotic constant is lower, approaching that computed in buoyancy preserving jets for $\Delta T_0 \approx 5$ °C.

Thus, the computed maximum terminal penetration depth is underestimated, while the computations give results that are close to the steady state terminal penetration depth. We were able to obtain the maximum penetration depth, by reducing the jet entrainment coefficient to a value around 0.025 (regarding Gaussian distributions).

The dimensionless buoyancy flux obtained numerically at different initial temperatures is depicted in Fig. 7. One may note that the smaller the temperature difference between jet and ambient fluid, the bigger the buoyancy flux at Z_{max}. For each initial temperature difference, the buoyancy at Z_{max} is increasing with R_0. This is evident since when $R_0 > 0.1$, mixing is reduced drastically. For $\Delta T_0 \approx 5$ °C the buoyancy flux is greater than 90% of the initial, at all initial flow Richardson numbers.

It would be interesting to examine the computed average dilution factor S at Z_{max}, that is the ratio of the volume flux of the jet at Z_{max}, over the initial discharge $S = \mu(Z_{max})/Q$. The dimensionless average dilution expressed as $SQ/z\sqrt{M}$ is plotted against R_0 in Fig. 8. At low initial Richardson numbers ($R_0 < 0.1$) the normalized dilution takes the value 0.285, while it increases with R_0 when $R_0 > 0.1$. The buoyancy preserving jets seem to dilute faster than the heated jets. Dilution data of hot water jets at different initial temperature differences collapse to a constant when $R_0 < 0.1$. The computations failed when $R_0 > 0.4$. In Fig. 9 we have plotted the dimensionless average centerline dilution computed from the data reported by Seban et al. [15] taken in negatively buoyant hot air jets, versus the normalized distance z/l_M from the source. In this graph one may observe two things: (i) the normalized time-averaged dilution at the centerline is constant with an average value of about 0.30–0.35 when $z/l_M < 1.75$, result that is close to the value 0.285 we have obtained at Z_{max} numerically for hot water

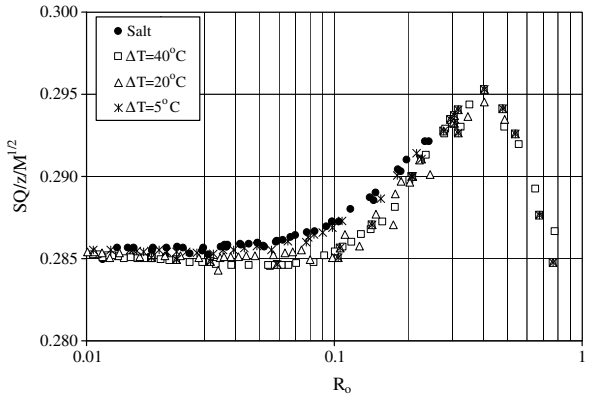

Fig. 8. Normalized average dilution predicted by the model at Z_{max} versus R_0 for saltwater jets (solid circles), and hot water jets at different initial temperature differences from ambient (open symbols).

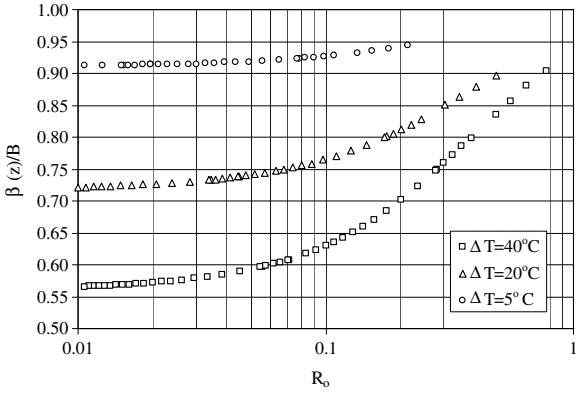

Fig. 7. Normalized buoyancy decay in a hot water jet, predicted by the model at Z_{max} versus R_0 at different initial temperature differences from ambient fluid.

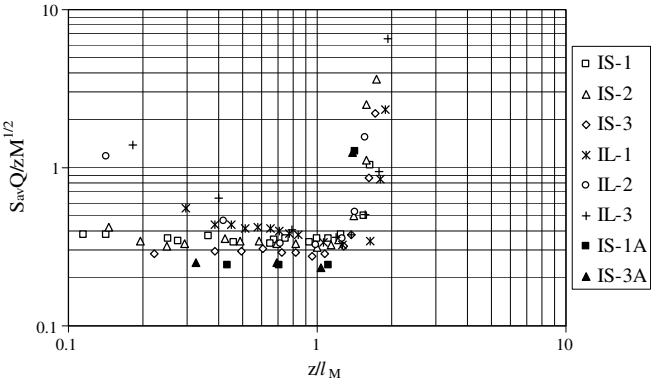

Fig. 9. Normalized average dilution at the centerline versus z/l_M, from data reported by Seban et al. [15].

jets. (ii) Once $z/l_M > 1.75$ the normalized average dilution becomes infinite, meaning that the temperature difference measured is quite low (measurement of intermittent jet-ambient air temperature). In summary, one may state that for negatively buoyant jets at $R_0 < 1$, an average dilution obtained can be computed from equation

$$S = \frac{\mu(z)}{Q} = 0.3\frac{z\sqrt{M}}{Q} = 0.3\frac{z}{l_Q}. \quad (18)$$

The corresponding constant in round vertical positively buoyant jets ($z/l_M < 1$) evaluated from the data by Papanicolaou and List [29] is $0.165 \times 1.4 = 0.23$ (the mean over the jet cross-section temperature is approximately 1.4 times lower than the one at the axis).

4. Conclusion

Turbulent fountains of buoyancy preserving fresh water buoyant jets into salt water, and hot water jets into cold water have been investigated experimentally. The results of earlier experiments have been plotted together in order to show the diversity of the evaluated experimental constants. Besides the initial conditions, there are two main sources of error in the measurement of the penetration depth, one that is a result of the optical technique used, and the other from boundary effects due to the tank size if compared to that of the jets. The experiments have been performed in a tank that is large enough, so it did not introduce considerable boundary effects to the jet flow field. The length characteristics have been measured from videos taken over the course of experiments, combining the flow shadowgraphs with two grids for better accuracy in the measurement.

The maximum Z_{max}/l_M and the steady state terminal normalized penetration Z/l_M for initially jet-like flows ($R_0 < 0.1$), were measured to be 3 and 2, respectively, regardless of the buoyancy preserving or non-preserving type of the flow. The results are in agreement with those reported by Demetriou [16] and Zhang and Baddour [17] regarding round jets. The same experimental constants were found for jets with square and equilateral triangular nozzles, with rounded corners. In the case of rectangular jet nozzles with 2:1 side ratio and rounded corners, the constants of proportionality have been found lower from the previous, meaning that this type of nozzle is more efficient as a mixing mechanism. This result is congruent with earlier findings by Konstantinidou and Papanicolaou [24] and Ho and Gutmark [25].

Numerical evaluation of Z_{max} was carried out for round jets applying the entrainment coefficients and the $1/e$ jet width ratios λ for jets and plumes reported by Papanicolaou and List [26], and considering them to be functions of the local buoyant jet Richardson number. Using exponential time-averaged velocity and density deficiency profiles, the constant C is found to be 1.78 (higher than 2 in heated jets), result which is not congruent with experimental data. Bloomfield and Kerr [20] have reported a value of 2.32 for the normalized maximum penetration depth, assuming top-hat velocity and density deficiency profiles that is different from 1.87 reported here. We were able to reproduce their results removing $\sqrt{\pi}$ from continuity equation, meaning that the error is due to an incorrect continuity equation. The constant of proportionality $C = 3$ can be obtained numerically, only with dramatic reduction of the jet entrainment coefficient to a value around 0.025.

The average dilution has been estimated to be proportional to the terminal elevation, with a constant of proportionality in the range 0.29 to 0.30–0.35, the first being a numerical estimate and the second an experimental value from the data of Seban et al. [15].

It would be of interest to investigate the velocity field of negatively buoyant jets, by means of particle image velocimetry. Thus one can verify the entrainment and jet width constants to be used, for numerical prediction of the terminal penetration depth, and the average dilution of turbulent vertical fountains, in a homogeneous calm ambient.

Acknowledgement

The technical support of E. Pappas and D. Karaberopoulos is highly appreciated.

References

[1] H. Rouse, C.-S. Yih, H.W. Humphreys, Gravitational convection from a boundary source, Tellus 4 (1952) 201–210.
[2] B.R. Morton, G.I. Taylor, J.S. Turner, Turbulent gravitational convection from maintained and instantaneous sources, Proc. Roy. Soc. London A234 (1956) 1–23.
[3] P.N. Papanicolaou, Mass and momentum transport in a turbulent buoyant vertical axisymmetric jet, Report No. KH-R-46, W.M. Keck Laboratory of Hydraulics and Water Resources, California Institute of Technology, Pasadena, California, 1984.
[4] H. Wang, A.W.-K. Law, Second-order integral model for a round turbulent buoyant jet, J. Fluid Mech. 459 (2002) 397–428.
[5] E.J. List, J. Imberger, Turbulent entrainment in buoyant jets and plumes, J. Hyd. Div., ASCE 99 (9) (1973) 1461–1474.
[6] W.P. Muellenhof, A.M. Soldate, D.J. Baumgartner, M.D. Schuldt, L.R. Davis, W.E. Frick, Initial Mixing Characteristics of Municipal Ocean Discharges, vol. 1, Procedures and Applications, EPA/600/3-85/073a, 1985, p. 90.
[7] I.R. Wood, R.G. Bell, D.L. Wilkinson, Ocean Disposal of Wastewater, World Scientific, 1993.
[8] G.H. Jirka, Integral model for turbulent buoyant jets in unbounded stratified flows. Part 1: single round jet, Env. Fluid Mech. 4 (2004) 1–56.
[9] J.S. Turner, Jets and plumes with negative or reversing buoyancy, J. Fluid Mech. 26 (1966) 779–792.
[10] G. Abraham, Jets with negative buoyancy in homogeneous fluid, J. Hyd. Res. 5 (4) (1967) 235–248.
[11] W.D. Baines, J.S. Turner, I.H. Campbell, Turbulent fountains in an open chamber, J. Fluid Mech. 212 (1990) 557–592.
[12] A.W. Woods, C.P. Caulfield, A laboratory study of explosive volcanic eruptions, J. Geophys. Res. 97 (1992) 6699–6712.
[13] J.S. Turner, I.H. Campbell, Convection and mixing in magma chambers, Earth Sci. Rev. 23 (1986) 255–352.
[14] I.H. Campbell, J.S. Turner, Fountains in magma chambers, J. Petrol. 30 (1989) 885–923.
[15] R.A. Seban, M.M. Behnia, K.E. Abreu, Temperatures in a heated jet discharged downward, Int. J. Heat Mass Transfer 21 (1978) 1453–1458.

[16] J.D. Demetriou, Turbulent diffusion of vertical water jets with negative buoyancy (In Greek), Ph.D. Thesis, National Technical University of Athens, 1978.
[17] H. Zhang, R.E. Baddour, Maximum penetration of vertical round dense jets at small and large Froude numbers, J. Hyd. Eng., ASCE 124 (5) (1998) 550–553, Technical Note No. 12147.
[18] W.R. Lindberg, Experiments on negatively buoyant jets, with and without cross-flow, in: P.A. Davies, M.J. Valente Neves (Eds.), Recent Research Advances in the Fluid Mechanics of Turbulent Jets and Plumes, NATO, Series E: Applied Sciences, vol. 255, Kluwer Academic Publishers, 1994, pp. 131–145.
[19] L. Pantzlaff, R.M. Lueptow, Transient positively and negatively buoyant turbulent round jets, Exp. Fluids 27 (1999) 117–125.
[20] L.J. Bloomfield, R.C. Kerr, A theoretical model of a turbulent fountain, J. Fluid Mech. 424 (2000) 197–216.
[21] H.B. Fischer, E.J. List, R.C.Y. Koh, J. Imberger, N.H. Brooks, Mixing in Inland and Coastal Waters, Academic Press, 1979.
[22] P.N. Papanicolaou, A piston driven jet for the study of the zone of flow establishment, Exp. Fluids 17 (1994) 287–289.
[23] T.J. Kokkalis, Vertical turbulent jets of negative buoyancy in a calm homogeneous ambient, M.S. Thesis, Hydromechanics and Environmental Engineering Laboratory, University of Thessaly, 2006 (In Greek).
[24] K. Konstantinidou, P.N. Papanicolaou, Vertical round and orthogonal buoyant jets in a linear density-stratified fluid, in: J. Ganoulis, P. Prinos (Eds.), XXX IAHR Congress Proceedings, Theme C, vol. 1, 2003, pp. 293–300.
[25] C.M. Ho, E. Gutmark, Vortex induction and entrainment in a small-aspect-ratio elliptic jet, J. Fluid Mech. 179 (1987) 383–405.
[26] P.N. Papanicolaou, E.J. List, Investigations of round vertical turbulent buoyant jets, J. Fluid Mech. 195 (1988) 341–391.
[27] R.C. Weast (Ed.), CRC Handbook of Chemistry and Physics, 66th ed., CRC Press, 1985–1986.
[28] C.H.B. Priestley, F.K. Ball, Continuous convection from an isolated source of heat, Quart. J. Roy. Meteor. Soc. 81 (348) (1955) 144–157.
[29] P.N. Papanicolaou, E.J. List, Statistical and spectral properties of tracer concentration in round buoyant jets, Int. J. Heat Mass Transfer 30 (1987) 2059–2071.